Zia *et al. Journal of Ovarian Research* (2025) 18:44
https://doi.org/10.1186/s13048-025-01635-0

Journal of Ovarian Research

RESEARCH Open Access

Ameliorative effect of *Fagonia indica*-coated chitosan nanoparticles on the ovulatory pattern in PCOS rat model

Threem Zia[1], Irfana Liaqat[1*], Khawar Ali Shahzad[2,3], Mushtaq Hussain Lashari[4], Dalia Fouad[5], Farid S. Ataya[6], Saman Alam[1] and Areeba Saeed[1]

Abstract

Background Polycystic ovarian syndrome (PCOS) with wide-range prevalence, affecting 5–18% of females of reproductive age, and its substantive role as a primary etiological factor in anovulatory infertility, with up to 80% of such cases attributed to this syndrome having particular significance.

Objectives The current research delineates the outcomes of a meticulous inquiry into the efficacy of *Fagonia indica*-coated chitosan nanoparticles (FICNPs) in ameliorating the prevalent and clinically consequential PCOS in female Wistar rats.

Methodology FICNPs were synthesized by using a methanolic extract of *F. indica* and chitosan via the ion gelatin method. The nuanced interplay of hormonal profiles, ovarian histology, and miRNA expression in response to FICNPs intervention was investigated. Notable findings include an obvious decrease in luteinizing (LH) and testosterone hormone levels with high-dose FICNPs-treated subjects (100 mg/kg) compared to their untreated counterparts.

Results Follicle-stimulating hormone (FSH) and prolactin levels were markedly decreased in the untreated PCOS rat models, whereas, histopathological examination revealed augmented oocyte diameters in FICNP-treated rats, suggesting pronounced improvements in ovarian morphogenesis and follicular maturation. Additionally, real-time quantitative PCR analysis revealed disparate miRNA expression profiles, prominently implicating rno-miR-30c-2-3p, rno-miR-146b-5p, rno-miR-486, and rno-miR-3586-3p in the therapeutic efficacy of FICNPs. Notably, the progeny of FICNPs-treated subjects (F1 generation) showed normalized ovulatory activity, substantiating the sustained therapeutic potential of FICNPs.

Conclusion Collectively, these findings underscore the auspicious promise of FICNPs as a paradigm-shifting therapeutic modality for mitigating the complex pathophysiology of PCOS, thereby addressing its formidable prevalence and clinical import, with the potential to surpass conventional pharmacotherapy modalities.

Keywords PCOS, *Fagonia indica*-coated chitosan nanoparticles (FICNPs), Ovulatory function, Follicle-stimulating hormone, miRNA expressions, F1 generation

*Correspondence:
Irfana Liaqat
Irfana.liaqat@gcu.edu.pk

Full list of author information is available at the end of the article

Introduction

PCOS is a widespread endocrine dysfunction that contributes to approximately 80% of infertility cases worldwide [1]. Polycystic ovaries, increased testosterone levels, and irregular menstruation are the hallmarks of this illness, which can result in complications like diabetes, obesity, and other health problems [2, 3]. Insulin resistance and elevated luteinizing hormone levels are key factors contributing to infertility in patients with PCOS, resulting in hyperandrogenism and ovarian cyst formation. Aberrant gonadotropin discharge and increased ovarian steroid production are associated with PCOS. When LH content exceeds FSH concentration, the ovaries produce more androgens [4]. In reality, androgen levels in patients' blood rise as a result of theca cells producing androgens in response to luteinizing hormone [5–7] (Fig. 1).

Numerous therapeutic modalities are available for treating infertility and polycystic ovary syndrome (PCOS), including medications such as cyclic progestins, anti-androgens, letrozole, clomiphene citrate, and metformin [8–10]. However, these medications may have adverse effects, which leads many patients and healthcare providers to consider herbal remedies as alternative [11–14]. *Fagonia indica (F. indica)*, a well-known herb or shrublet of the Zygophyllaceae family, has been traditionally used for centuries to address menstrual issues and shows promising therapeutic potential due to its antioxidant, antitumor, anti-inflammatory, antihemorrhagic, antidiabetic as well as anti-ulcer properties [15, 16]. It is important to note that herbal extracts may require considerable time to produce significant results. As the majority of biologically active ingredients in herbal extracts, including flavonoids (quercetin), tannins, and terpenoids, are highly soluble in water but have poor absorption because they cannot pass through cell lipid membranes, have too large of a molecular size, or are poorly absorbed, which reduces their bioavailability and ability to work. As a result, these extracts take more time to produce noticeable effects [17].

Recent advancements in drug delivery technologies have incorporated chitosan nanoparticles and eco-friendly approaches utilizing phyto-medicines [18]. Chitosan can stick to mucosal surfaces and temporarily open tight junctions in mucosal cell membranes, it has an absorption-promoting effect. By extending the

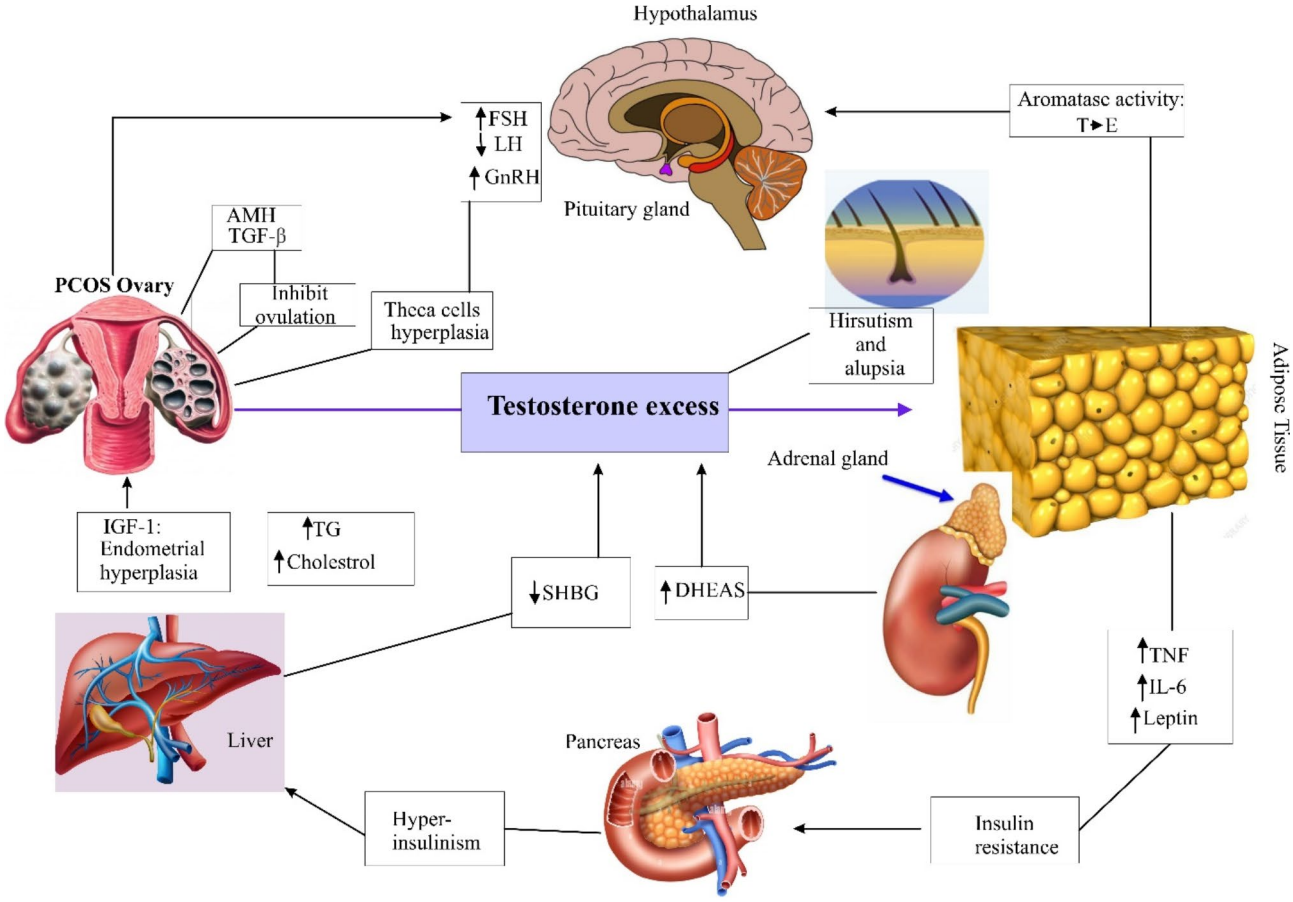

Fig. 1 Schematic sketch of PCOS pathophysiology exhibiting hormonal imbalance and inhibition of ovulation due to testosterone excess and physiological changes in ovaries

duration of contact between the medication and the absorptive surface, the interaction between negatively charged mucin and positively charged chitosan improves absorption [19]. Additionally, "chitosan nanoparticles" offer advantages such as small size, quantum size effects, and improved dispersion in biological systems. Furthermore, the non-toxic, biodegradable, and antibacterial characteristics of chitosan mark it a popular choice for applications of drug delivery [20]. Combining chitosan with substances like sodium tripolyphosphate (TPP) in nanoparticle form has shown promise in attenuating symptoms associated with conditions such as polycystic ovulatory activity. The ability of chitosan to enhance medication transport mechanisms underscores its value in developing innovative drug delivery techniques [21].

The main objective of the study was to create and evaluate biologically active compounds found in Sodium Tripolyphosphate (TPP) cross-linked chitosan nanocomplexes derived from methanolic leaf extracts of *F. indica*. These compounds were then assessed for their efficacy in protecting against "Estradiol Valerate (EV)"-induced PCOS in female rats by examining gonadotropin levels and observing ovarian histopathological changes. Moreover, this study sought to determine miRNA levels in various treatment groups to utilize miRNAs as noninvasive biomarkers for the early detection of PCOS. Rats that received effective treatment were carefully selected, and their first filial generation (F1 generation) was examined for further histological, hormonal, and molecular analyses. *F. indica*-coated Chitosan Nanoparticles (FICNPs) treatment can help to improve ovulatory activity and reduce infertility.

Materials and methods

Materials

Model wistar rats and reagents

In this study, female Wistar rats weighing an average of 150–170 g and aged 7–9 weeks were employed, as indicated in Table 1 [22]. *Inclusion Criteria for study* is, selection of adult female rats with normal estrous cycle, average weight (not obese), normal ovulatory pattern, without any prior disease symptoms were selected, divided into different groups for disease induction. While exclusion Criteria for study *is* female rats with already abnormal estrous cycle, showed the symptoms of any disease and weight below average were excluded from study. The rats were reared in Department of Zoology at Government College University Lahore and kept in an animal house during 48-hour acclimatization period. They were provided with appropriate food and maintained at standard temperature and humidity levels throughout the experimental period [6]. All animal experiment and method used was carried out in compliance with international standards and the Government College University's ethical research committee's recommendations (Letter number. GCU/IB/813). Low-molecular-weight chitosan ("CAS Number: 9012-76-4") was obtained from Sigma-Aldrich, MO, USA. Sodium tripolyphosphate (TPP) was procured from Sigma-Aldrich (CAS Number: 7758-29-4). MO, USA Estradiol valerate was provided as 2 mg/kg tablets (Estranor, Saffron, Pakistan), which stops regular ovulation [23]. Smooth-tipped pipettes were purchased from Sartorius, Singapore. Phosphate Buffer Saline (PBS) was prepared by adding 800 ml of distilled water, 8 g of NaCl, 1.44 g of Na_2HPO_4, 0.2 g of KCl, 0.24 g of KH_2PO, maintaining the pH to 7.2 and adding distilled water until the total volume reaches 1 L. Formalin was purchased from Chemworld International, Ltd., USA. TRIzol reagent was obtained from Invitrogen, USA (Catalog number: 15596026).

Collection of F. indica

The herb was collected from the local desert areas of Bhakkar (Pakistan). It belongs to the Zygophyllaceae family. It was recognized and authenticated by the botanist, Dr. Zaheer ud din Khan at Government College University Lahore and for further reference, it was preserved under specimen number 056-62-02 in the Dr. Sultan Ahmed herbarium of the Department of Botany (GCU Lahore) for further reference. The leaves are separated from the plants and then dried for powder synthesis.

Methodology

Synthesis of F. indica-loaded chitosan nanoparticles

FICNPs were fabricated following an established green synthesis method [24]. Briefly, finely sieved and dried 100 g of *F. indica* leaves were subjected to Soxhlet equipment for the production of a methanol extract. The

Table 1 Rat body weight values representing mean ± sem. [a-e] within the same row, means with different superscripts are significantly different ($p < 0.05$)

Time intervals	Number of rats	Group-I	Group-II	Group-III	Group-IV	Group-V	Group-VI	*P* Value
Day 1	5	166.7 ± 0.38	170.6 ± 0.74^{b}	168.8 ± 0.42^{c}	171.5 ± 0.39^{cd}	165.7 ± 0.38^{d}	175.7 ± 0.40^{d}	0.00
Day 7	5	171.2 ± 0.25^{a}	181.4 ± 0.65^{b}	173.2 ± 0.25^{a}	168.8 ± 0.42^{c}	171.2 ± 0.38^{c}	183.9 ± 0.42^{c}	0.00
Day 14	5	179.0 ± 0.23^{a}	189.1 ± 0.60^{d}	180.6 ± 0.44^{e}	172.5 ± 0.34c	179.4 ± 0.30^{d}	191.7 ± 0.34^{d}	0.00
Day 21	5	184.8 ± 0.20^{a}	201.2 ± 0.42^{de}	193.5 ± 0.32^{e}	209.1 ± 0.42^{ab}	188.8 ± 0.31^{cd}	210.8 ± 0.30^{bcd}	0.00

Note: [a–e] Within the same row, means with different superscripts are significantly different ($p < 0.05$)

extract was baked at 40 °C after being dried for 15 to 20 min in a rotary evaporator. The ion-gelation method was utilized for the formation of nanoparticles, with sodium tripolyphosphate (TPP) serving as an agent for cross linkage [25].

Chitosan nanoparticles were prepared using leaves extract, and "sodium tripolyphosphate (TPP)" was used as a crosslinking substance. The plant extract (1.5% w/v) was prepared by methanol extraction and added separately to 0.5% w/v TPP under gentle magnetic stirring at room temperature. The solution was then added dropwise to a chitosan solution with 2% v/v acetic acid and 1% w/v chitosan. The solution was then added dropwise into chitosan solution with 2% v/v acetic acid and 1% w/v chitosan. The solution was sonicated at 80 amplitudes and centrifuged at 8000 rpm for 20 min. The pellet was then lyophilized into powder form.

Characterization of nanoparticles

Ultraviolet-visible spectroscopy (UV), Fourier transform infrared spectroscopy (FTIR), and X-ray diffraction (XRD) were used to characterize the prepared FICNPs. These analyses were performed at the "Center for Advanced Studies in Physics (CASP Laboratory GCU, Lahore)". Ultraviolet-visible (UV-Vis) spectroscopy was used to ensure the fabrication of desired material (UV-1900i, USA) [26]. The absorbance of the FICNPs was in the range–200–400 nm.

High spectral resolution data over a broad-spectrum range were concurrently acquired by the FTIR spectrometer. This offers a notable benefit in comparison to a dispersive spectrometer, which gauges intensity concurrently across a limited range of wavelengths. To investigate the interactions between the functional groups of chitosan, *F. indica*, and FICNPs, FTIR was employed using the FTIR model (IRPrestige-21, USA) as previously described [27].

A Cu Kα radiation-equipped X-ray diffraction (XRD) spectrum (Bruker, D2 Phaser, USA) with an average wavelength of 1.54059 Å was used to assess the mean crystal size, phase composition, and other structural details of the nanoparticles. A computerized library was used to identify target materials by comparing the positions and intensities of the peaks. The XRD profile was also affected by the NP dimensions. Large-sized materials show tapered peaks, whereas small-sized materials show broad peaks [27].

Rat rearing and PCOS induction

The PCOS rat model was prepared as previously described [28] with minor modifications. Female Wistar rats with a typical four-phase estrous cycle were injected intraperitoneally with estradiol valerate (2 mg/kg) dissolved in 0.1 mL of corn oil (a single dose) for induction of PCOS and assessed for 30 days. Total 30 PCOS rats were divided into six groups ($n = 5$) at random, and each group was given a number label that indicated where it belonged. Female rats in Group 1 served as negative controls, while those in Group 2 were affected by PCOS (positive control). Group 3 received standard metformin treatment (28 mg/kg) (standard control group), while Group 4 was treated with *F. indica* (500 mg/kg) (treatment group 2). Group 5 received a low dose of FICNPs (50 mg/kg) (treatment group 3), and Group 6 was treated with a high dose of FICNPs (100 mg/kg) (treatment group 4). The treatment of PCOS with *F. indica*, FICNPs, and standard drug metformin in respective groups was followed for 28 days with the oral administration of drugs on a daily basis. The schematic layout of PCOS induction and treatment is shown in Table 2; Fig. 2.

Analysis of vaginal smears

Rats were subjected to vaginal smear examinations to determine their estrus stages. Vaginal smears were collected before (day 0), during (days 14) and after the induction of polycystic ovarian syndrome (PCOS), (day 28) as well as at the end of the treatment period (30 days) to assess the regularity of the estrous cycle, which is disrupted by PCOS [29]. The estrus cycle of the rats was assessed by preparing vaginal smear slides using the vaginal lavage protocol [30, 31]. Briefly, a smooth-tipped pipette with a 1.5 mm bore size was employed to draw 0.1 mL of PBS, which was inserted 1–2 mm deep into the rat's vaginal orifice and flushed 2–3 times inside and outside the vagina for cytology. The smear was placed on a slide and permitted to dry at room temperature (RT). The smear was fixed by covering it with a few drops of methanol followed by Giemsa stain. The slides were washed with tap water, stained again with a diluted Giemsa stain, and observed under a microscope at 40× magnification after washing and air-drying [32].

Euthanization, blood and organ collection

After completing the 28-day treatment regimen of all 6 groups, rats were humanely euthanized on diestrus stage, using a cervical dislocation procedure under anesthesia with 3-5% isoflurane mixed with oxygen. Blood and organ samples were obtained from all the rats in the different treatment groups. Blood samples were collected via a heart puncture. Serum was obtained from blood samples that were centrifuged for 15 min at 3000 rpm after placing samples 4 h at room temperature. The serum was then kept at -20 °C for use in additional experiments. Rat ovaries were stored in 10% buffered formalin for further analysis such as H & E staining [33].

Table 2 Representing the methodology of experiment for PCOS induction and treatment phase

Sr. No	Groups	Duration (8 weeks)
1	**Dosing schedule during the disease induction phase**	
	1. Normal control (N.C)	Normal rat diet and water
	2. Disease control (Diseased, untreated)	Estradiol valerate (EV) was injected intra-peritoneally (2 mg/kg) dissolved in 0.1 mL of corn oil (a single dose) to induce PCOS
2	**Dosing schedule during the treatment phase**	
	1. Normal control (N.C)	Normal rat diet and water
	2.Disease control (Diseased, untreated)	Normal rat diet and water
	3.Standard metformin 28 mg/kg	Metformin 28 mg/kg was administered to EV induced PCOS rats
	4. *Fagonia indica* (F. indica) 500 mg/kg	Treated with *F. indica* (500 mg/kg) herbal extract
	5. Low dose of *Fagonia indica coated* chitosan nanoparticles(FICNPs) (50 mg/kg)	Treated with low dose of *F. indica coated chitosan nanoparticles* (50 mg/kg)
	6.High dose of FICNPs 100 mg/kg	Treated with high dose of *F. indica coated chitosan nanoparticles* (100 mg/kg)
3	**After treatment Phase (First Filial Generation)**	
	1.Three rats from group 3 (Standard metformin 28mg/kg) paired with normal male rats (1:1)	Feed with normal rat diet and water without any treatment for F1 generation studies
	2. Three rats from group 6 (treated with high dose of FICNPs 100 mg/kg) paired with normal male rats (1:1)	Feed with normal rat diet and water without any treatment for F1 generation studies

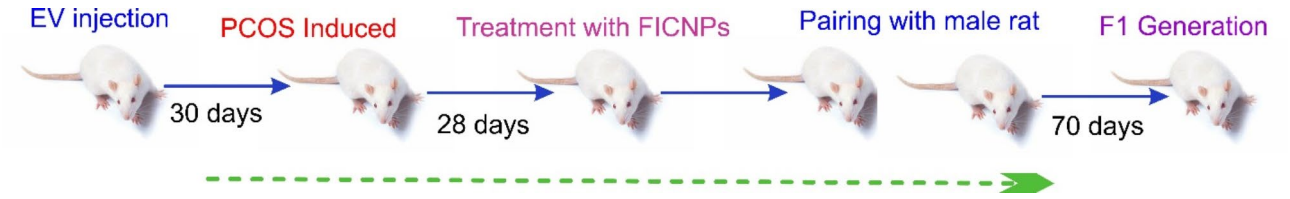

Fig. 2 Model representing the experimental layout from stage 1 to stage 5 i.e., PCOS induction (estradiol valerate (EV) injection; single dose), treatment with *F. indica* chitosan nanoparticles (FICNPs) (on daily basis), pairing with healthy male rats and finally F1 generation

Biochemical analysis

The collected serum samples were examined for "luteinizing hormone" (LH), "follicle stimulating hormone" (FSH), prolactin (PRL) and testosterone levels using commercially available assays (Invitrogen Elisa kits from Thermo Fisher Scientific, Cat #EEL121l, Cat #EEL125and Cat #ERA50RB, respectively. The manufacturer's instructions for using enzyme-linked immunosorbent test (ELISA) kits were followed. As previously reported, a standard curve was used to quantify the hormone concentration [33].

Slide Preparation for histology

The ovarian tissues were embedded in durable paraffin wax for preservation. A rotary motorized microtome (Myr EC-350-1, Spain) was utilized to slice the tissue paraffin into 3 µm thin ribbons for analysis. The ribbons were subsequently put on a glass slide, hematoxylin and eosin (H&E) were used for staining and slides were observed for histopathological changes [34]. A light microscope (LABOMED® USA) was used to examine each slide. Histomorphometry was performed using a commercial tool called Prog Res®2.1.1 Capture Prog Camera Control Software.

Sample isolation and storage

For ovarian tissue isolation, made a small incision in the abdominal walls of rats and located the ovaries. Gently isolate the ovaries with forceps, ensuring minimal contamination from surrounding tissues. Rat ovaries were stored in 10% buffered formalin and stored tissue samples at **-80 °C** until further processing for RNA extraction.

RNA and miRNA isolation using trizol reagent

Total RNA, including miRNA, was extracted from the samples using the **TRIzol reagent** (Invitrogen, Cat. No. 15596026) according to the manufacturer's protocol [35].

Step I: Homogenization of Samples

Tissue were homogenized in **1 mL of TRIzol reagent** per 100 mg of tissue or 1 × 10^6 cells. This was done using a syringe to ensure complete disruption of the tissue/cell membrane.

Step II: Phase Separation

After homogenization, **0.2 mL of chloroform** was added to the homogenate, and the mixture was vigorously shaken for 15 s. The sample was then incubated at room temperature for 3 min. The sample was centrifuged at **12,000 x g for 15 min** at 4 °C. This resulted in phase separation: The **upper aqueous phase** contained

the total RNA, including miRNA. The **interphase** contained DNA, and the **organic phase** contained proteins and lipids.

Step III: RNA Precipitation

The aqueous phase was carefully transferred to a new tube, and **0.5 mL of isopropanol** was added to precipitate the RNA. The sample was mixed well by inversion and incubated at **-20 °C for at least 1 h** or overnight to enhance RNA precipitation.

Step IV: RNA Wash

Following incubation, the RNA was pelleted by centrifugation at **12,000 x g for 10 min** at 4 °C.The RNA pellet was washed with **1 mL of 75% ethanol**, mixed gently, and then centrifuged at **7,500 x g for 5 min** at 4 °C.

Step V: RNA Re-suspension and Quality Assessment

The RNA pellet was air-dried for 5 min and re-suspended in **RNase-free water** or an appropriate buffer. RNA concentration and purity were assessed using a **NanoDrop 8000 spectrophotometer** (NanoDrop, Wilmington, DE, USA). RNA purity was confirmed by ensuring the A260/A280 ratio was between 1.8 and 2.0. The integrity of the RNA was checked via gel electrophoresis [36].

cDNA synthesis

A total of **250 ng of purified RNA** from each sample was reverse-transcribed to complementary DNA (cDNA) for downstream **Thermo Fisher Scientific**, **Cat. No. 4,368,814.** The procedure was as followed. For each reaction, **2 µg of isolated RNA** was used. The RNA was reverse-transcribed into cDNA using the Thermo Fisher kit, following the manufacturer's guidelines for enzyme activity and reaction setup [37].

Real time quantitative PCR (RT-qPCR)

RT-qPCR was performed using an ABI Step One Plus Real-Time PCR System (Applied Biosystems, USA) using SYBR Green PCR Master Mix (Thermo Fisher Scientific, Inc.) following the manufacturer's guidelines [38]. The sequences of the primers used were mentioned in Table 3 of revised manuscript. PCR amplification was carried out with an initial denaturation step at 95 °C for 30 s, followed by 40 cycles of 95 °C for 10 s (denaturation) and 60 °C for 20 s (annealing). The expression levels of the target genes were normalized to the housekeeping gene GAPDH, and data analysis was performed using the comparative $2^{-\Delta\Delta Cq}$ method for miRNA relative expression level analysis [38].

Table 3 The primers used for genes and MiRNAs expression analysis

Name	Primer Sequence
GLUT4	(F) 5′-GATCGGCTCTGAAGATGGGG-3′ (R) 5′-GGAGGAAATCATGCCACCCA-3′
PTEN	(F) 5′-AGACCATAACCCACCACAGC-3′ (R) 5′-CAGGGCCTCTTGTGCCTTTA-3′
miR-30c-2-3p	(F) GCTGGGAGAAGGCTGTT (R)TGTCGTATCCAGTGCAGGGTCCGAG GTATTCGCACTGGATACGACAGAGTA
rno-miR-146b-5p	(F) GGGTGAGAACTGAATTCCA (R)TGTCGTATCCAGTGCAGGGTCCGAGG TATTCGCACTGGATACGACACAGCC
rno-miR-486	F: GGGGATACTAGACTGTGAGCT R: TGTCGTATCCAGTGCAGGGTCCGAGG TATTCGCACTGGATACGACTCGAGG
GAPDH	F: GGTATCGTGGAAGGACTCATGAC R: ATGCCAGTGAGCTTCCCGT TCAGC

First filial generation (F1 generation)

Four female Wistar rats were chosen from Group 3, which served as a standard control group, and Group 6, which treated with a high dose of FICNPs (100 mg/kg) and demonstrated highly significant outcomes. These female rats were paired with normal male Wistar rats for mating (1:1) in order to avoid interbreeding. The remaining female rats were euthanized for histological analysis, as per standard protocol [39]. After mating, female offspring were allowed to grow for 11 weeks, during which time they were fed a normal diet without any treatment. Following this period, the female offspring were separated and their estrous cycles were monitored. Biochemical analysis was conducted, followed by sacrificing the rats and performing histological and molecular analyses of their ovaries.

Statistical analysis

The statistical analysis was conducted with the help of (SPSS) version 17. Data are presented as mean ± SEM. 1-Way-ANOVA, or one-way analysis of variance, was used to analyse the data. The group differences of control, untreated and treated groups were compared by the Duncan Multiple Range Test (DMRT) for body weight and ovarian weight, and histomorphometric parameters (Granulosa cells, oocyte and antral diameter). Changes between the treated and untreated groups were considered significant at $p < 0.05$.

Results

Successful fabrication and validation of FICNPs by UV-visible spectrum

The detection of absorption peaks in the UV-visible spectrum provides evidence of the presence of the targeted biomolecules [40]. The nanoparticles in question exhibited a surface plasma resonance peak in the range of 300–450 nm when subjected to light of a specific wavelength using a UV–visible spectrophotometer (Fig. 3). The emergence of this peak validates the successful synthesis of *F. indica* nanoparticles in conjunction with chitosan. It is noteworthy that the FICNPs exhibited stability and remained non-agglomerated.

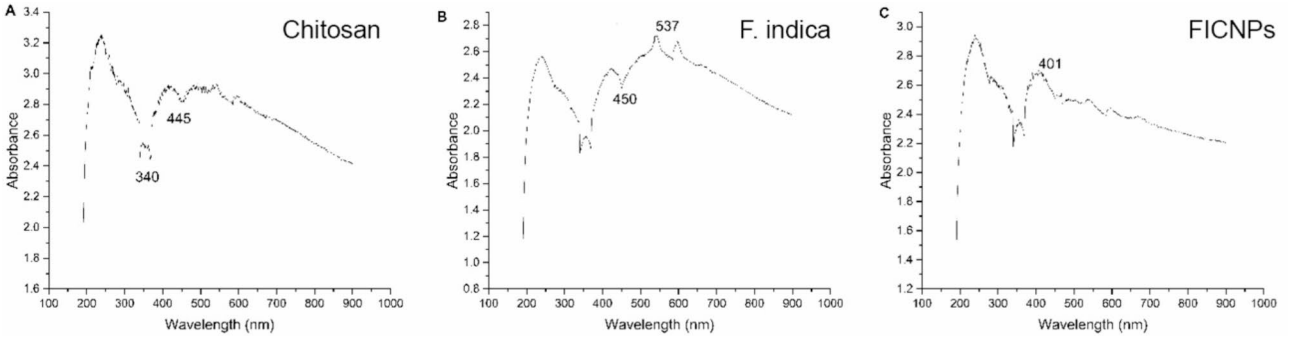

Fig. 3 UV-visible spectra showing different peaks in chitosan (**A**), *F. indica* (**B**), and *F. indica* chitosan nanoparticles (FICNPs) (**C**)

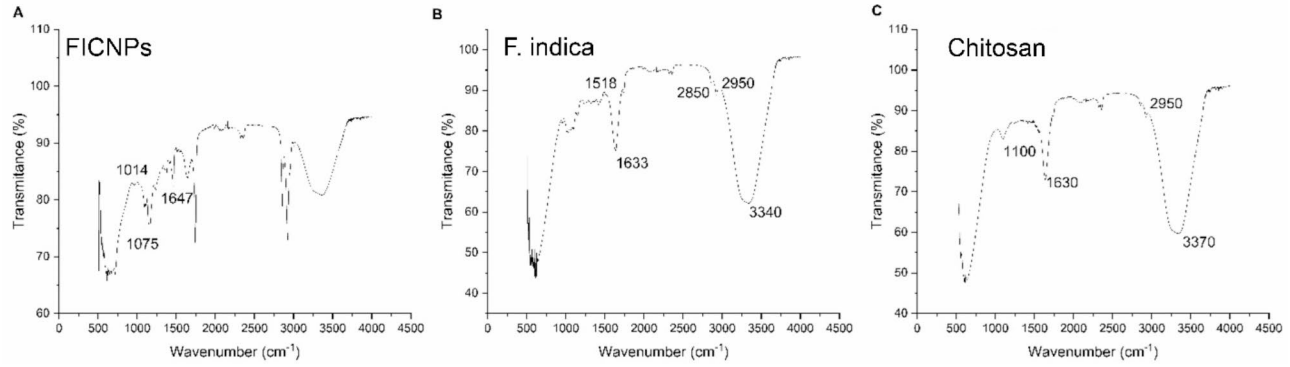

Fig. 4 Fourier transmission infrared radiation (FTIR) analysis of (**A**) *F. indica* chitosan nanoparticles (FICNPs) (**B**) *F. indica* and (**C**) chitosan showing peaks for different chemical bonds as discussed in text

FTIR spectrum

FTIR Spectrum analysis was performed to the exam the structures and study of chemical interactions between the functional groups of various components. Infrared analysis of chitosan showed a broad absorption band at 3370 cm^{-1}, which was attributed to the stretching of O-H and N-H [41]. The bands at 1633 and 1518 cm^{-1} correspond to the axial C = O stretching of the acetamido groups (amide I) and N-H bending vibrations, respectively, coinciding with the amide II vibration. The band at 3340 cm^{-1} in the chitosan spectrum corresponds to the -OH stretching vibration associated with the stretching vibration of the N-H group. The peak at 3339.35 cm^{-1} in the FTIR spectrum of the *F. indica* leaf extract could be attributed to the stretching vibration of both primary and secondary amines or to the -OH and -NH functional groups. The strong peaks at 2950 and 2850 cm^{-1} were attributed to alkane C-H symmetric and asymmetric stretching vibrations, respectively. The presence of amide C = O stretching is indicated by the peaks at 1646.76 and 1642.85 cm^{-1}. The C-O-C stretching vibrations may be responsible for the two strong and intense peaks at 1014.15 and 1075.79 cm^{-1} (Fig. 4).

XRD analysis

X-ray diffraction (XRD) analysis was used to elucidate the crystalline structure of the samples based on their physical properties. XRD was conducted to investigate the crystalline structure [42]. The XRD pattern of the *F. indica* nanoparticles combined with chitosan exhibits that the material exhibited semi-crystalline to crystalline characteristics following nanoparticle formation (Fig. 5).

FICNPs treatment restored the vaginal cell morphology and estrous cycle in rat model

The estrous cycle abnormalities in rats before and after PCOS induction were examined using both positive and negative controls in the study. Hormonal imbalances or pregnancy can interrupt the estrous cycle, which normally lasts four to five days. The cycle is characterized by four distinct stages of vaginal cell morphology and the restoration of the cycle was evaluated by comparing the ratio of leukocytes and nucleated to cornified enucleated squamous epithelial cells. In PCOS-induced rats with a dominant diestrus stage, the estrous cycle was disrupted and at metestrus stage with cornified epithelium, nucleus and neutrophils were shown. Whereas the FICNP-treated group exhibited noteworthy restoration

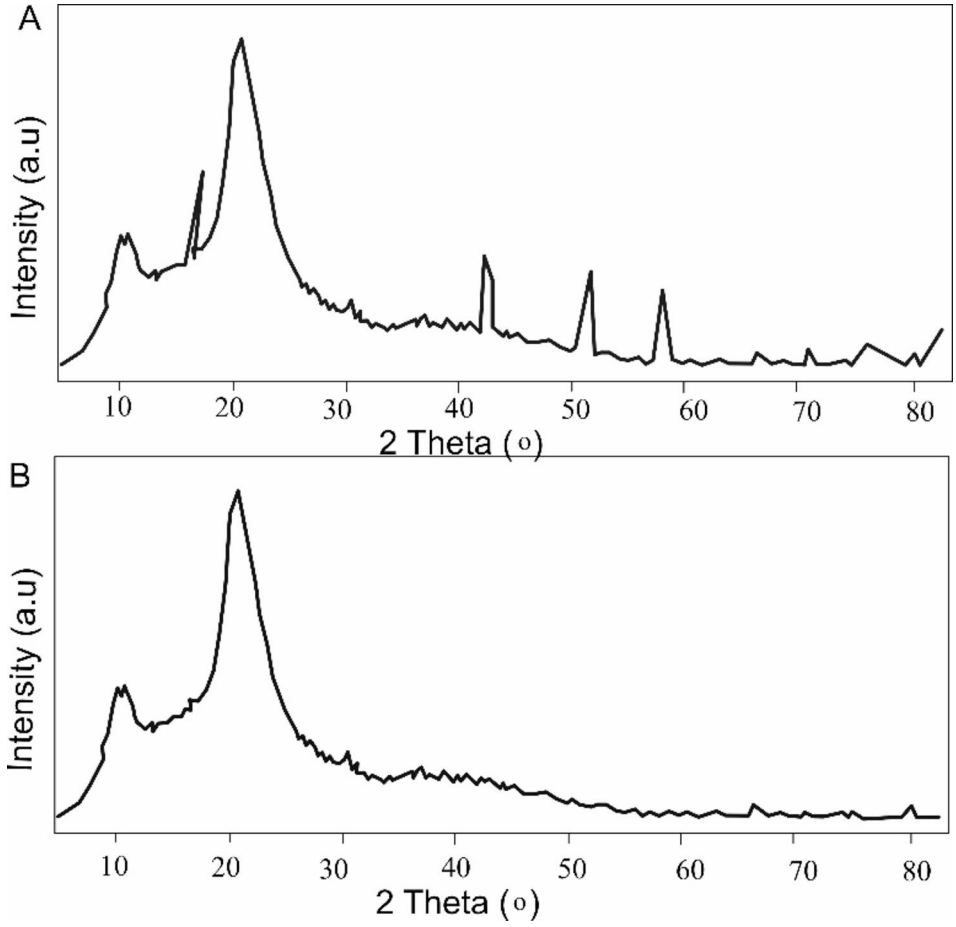

Fig. 5 The X-ray diffraction peaks of (**A**) *F. indica* chitosan nanoparticles (FICNPs) and (**B**) chitosan showing semi-crystalline to crystalline structure

of estrous cycle, indicating its effectiveness in treating PCOS-induced estrous cycle disruption (Fig. 6).

The F1 offspring from both groups, namely the metformin-treated and FICNP-treated groups (100 mg/kg), exhibited normal vaginal cell morphology, estrous cycle with normal four stages. No irregularities were detected in the vaginal smear cytology after 28-days.

FICNPs treatment ameliorated the metabolic and hormonal disturbances in PCOS Wistar rats

F. indica has demonstrated its potential to ameliorate the metabolic and hormonal disturbances that are characterized by PCOS. The main factor for LH hypersecretion in anovulatory patients is imbalanced negative feedback on LH secretion, which is mediated by progesterone or estradiol [43]. The levels of LH were significantly higher (5 mIU/mL) in the untreated PCOS group compared to the control group (4.1mlU/mL). Rats treated with FICNPs (high dose, 100 mg/kg) exhibited considerably lower LH levels (4.4 mlU/mL). The levels of FSH and prolactin were considerably lower in the PCOS group in comparison to the control group (FSH: 6 mlU/mL, Prolactin: 34 ng/mL). In all treatment groups, the levels of FSH and prolactin were noticeably elevated compared to those in the control group (FSH: 5.8 mlU/mL, Prolactin: 32 ng/mL). Nonetheless, the FICNPs group's levels of prolactin and FSH did not differ statistically from those of the metformin-treated group ($p > 0.05$). Testosterone levels in normal control was 2.8nmol/L and in untreated PCOS rats was 4.0 nmol/L which is significantly higher than control group. In the FINCNPs (100 mg/kg)-treated group, the level was 2.9 nmol/L which was significantly lower than that in the PCOS group, while metformin was not significantly different from the FICNP-treated group. Hormonal levels in the F1 generation were not significantly different from control group Fig. 7).

High dose FICNPs treatment vanished the multiple cysts, and restored the normal follicular growth

PCOS is a syndrome that disturbs the normal development of follicles. In PCOS, follicles are arrested at their immature stage, and the process of determining a dominant follicle does not occur [41]. In contrast, the ovaries of the control group exhibited well-defined oocytes, follicles, follicular fluid, and proliferating follicles with a single layer of flat granulosa cells encircling the oocytes.

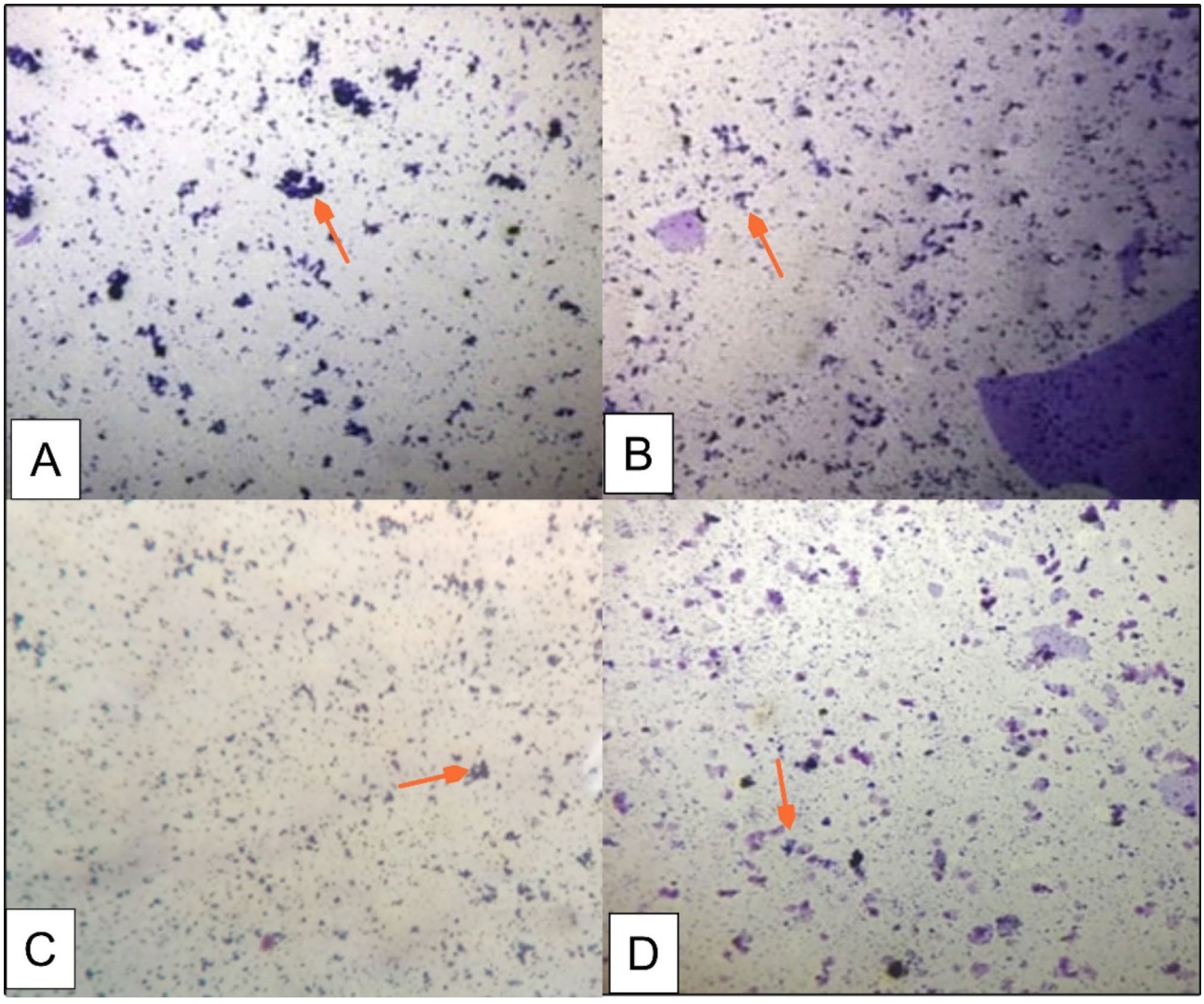

Fig. 6 (**A**) Control group in diestrus stage with some cornified epithelium; (**B**) PCOS rat group; in metestrus stage with cornified epithelium with nucleus and neutrophils (**C**) Metformin treated group showing diestrus stage with cornified epithelium (**D**) *F. indica* coated chitosan nanoparticles (FICNPs) treated group; at diestrus stage with cornified epithelium

Secondary follicles, which have two or more layers of granulosa cells, contain oocytes at the mid-growth stage. In the untreated PCOS group, a considerable percentage of transitory endocrine corpus luteum is present, and the ovaries are cystic and disorganized. Metformin treatment resulted in normal follicular growth, a decline in the proportion of cystic structures, and an increase in the corpus luteum ratio. Curing PCOS with *F. indica* extract (500 mg/kg) caused the growth of follicles and corpus luteum and the development of primordial follicles. Low doses of *F. indica* chitosan nanoparticles (50 mg/kg) restored follicular development and caused the polycystic tumors to disappear. When PCOS was cured with high doses of *F. indica* chitosan nanoparticles (100 mg/kg), histological examination of the ovaries revealed that multiple cysts had vanished, and normal follicular growth had begun. The corpus luteum was also recovered, and the ovaries exhibited a thick granulosa layer, well-developed oocytes, a clear antrum surrounding the oocyte, and a mature central oocyte and zona pellucida encasing the egg cells (Fig. 8).

The ovaries from the F1 generation of group 3 (treated with metformin) displayed interstitial and thick granulosa cells, as well as the presence of primordial follicles (PF) and normal oocyte synthesis. In accordance, the ovaries from group 6 (FINCNPs 100 mg/kg) exhibited normal stromal cells (SC) but showed degeneration of primordial follicles. Additionally, the ovarian sections revealed the presence of granulosa cells (GC) and deformed follicle cells (DFC).

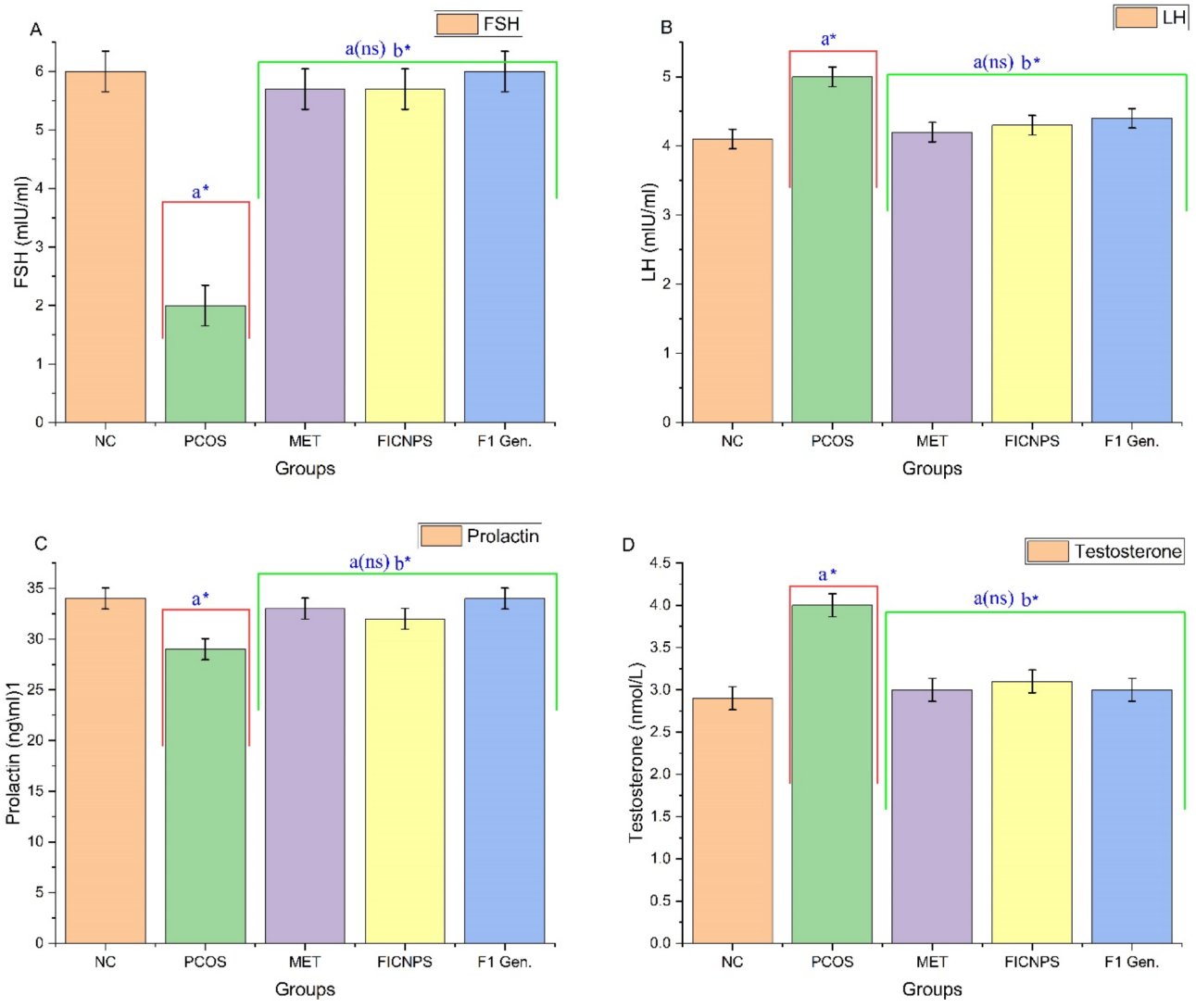

Fig. 7 (**A**) Luteinizing Hormone (LH) (**B**) Prolactin and (**C**) Follicle Stimulating Hormone (FSH) levels in the control and treatment groups are graphically represented. All the experiments were repeated in triplicates. One-way ANOVA and TMRT were used to analyze the data, which gave Mean + SEM. Significant differences between PCOS and the other categories are indicated by asterisk. Normal control (NC); a, PCOS group; b, ns; non-significant, asterisk; ($^{*}p < 0.05$)

Increased oocyte diameter, Thick granulosa cell layers and normal antral diameter was observed in FICNPs treated female rats and there F1 generation

In group 6, FICNPs (100 mg/kg), the granulosa cells in these groups were significantly thicker than those in the control and other treatment groups ($P \leq 0.05$). When the positive control and standard (metformin) groups were compared, the oocyte diameter was increased in all treated groups; however, a significant increase was observed in the FICNPs (100 mg/kg)-treated groups. The antral diameter, as measured by histomorphometry, was larger in the FICNPs group than in the control group (Table 4).

The F1 generation of group 3 and 6 (metformin-treated, FICNPs 100 mg/kg) also displayed increased oocyte diameter, thick granulosa cell layers, and normal antral diameter. Furthermore, the histomorphic characteristics of the F1 generation were consistent with those of the control group in all aspects.

FICNPs treated rats showed potential therapeutic benefits in improving MicroRNA dysregulations

The present study presents significant findings regarding the miRNA expression profiles of first-filial generation (F1) individuals in the context of PCOS. In particular, miR-141-3p is significantly downregulated in PCOS subjects, which is associated with disrupted glucose and lipid metabolism, possibly through PTEN regulation [44, 40]. Relative mRNA levels of genes (PTEN and GULT4) significantly downregulated in PCOS-induced rats

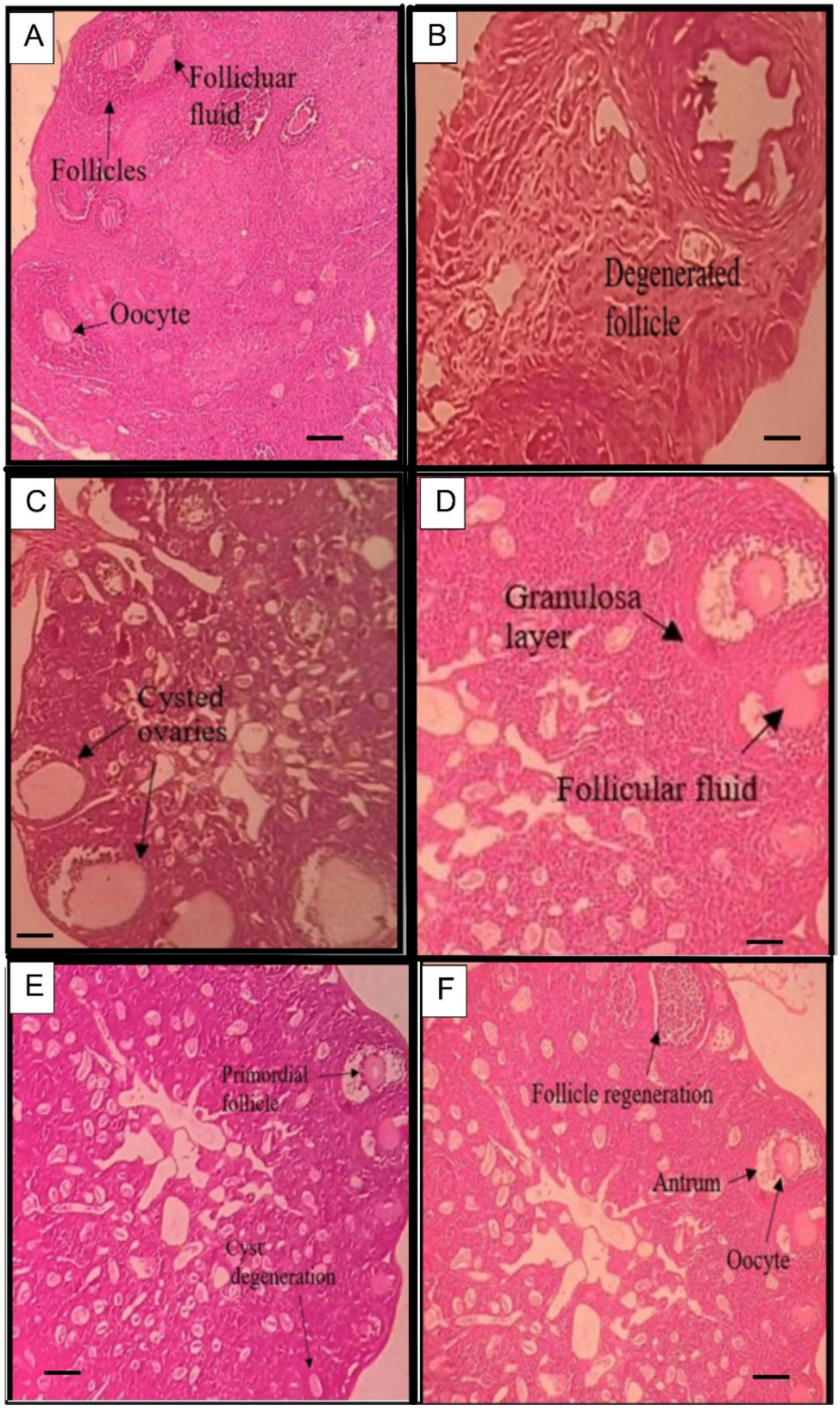

Fig. 8 H &E micrographs of ovaries (**A**) Control group; showing normal oocytes, (**B-C**) PCOS rat group; Showing cysts in ovaries and degenerated follicles (**D**) Metformin treated group showing again, normal oocyte formation and thick granulosa (**E**) *F. indica* coated chitosan nanoparticles (FICNPs) treated group; regenerating primordial follicles and cyst degradation (**F**) F1 generation; showing normal oocytes follicle regeneration and antrum, scale; bar 40×

Table 4 Morphometric analysis of ovarian weight histology, values represent the mean ± sem of 6 groups

Parameters	NC	PCOS	Metformin	F. indica (500 mg/kg)	FICNPs (50 mg/kg)	FICNPs (100 mg/kg)
Ovarian Weight(g)	$0.15^{e} \pm 0.01$	$0.26^{b} \pm 0.02$	$0.14^{e} \pm 0.01$	$0.16^{e} \pm 0.01$	$0.17^{e} \pm 0.01$	$0.13^{e} \pm 0.01$
Granulosa cells	$0.01^{e} \pm 0.00$	$0.05^{a} \pm 0.00$	$0.01^{e} \pm 0.00$	$0.04^{b} \pm 0.00$	$0.04^{b} \pm 0.00$	$0.02^{d} \pm 0.00$
Oocyte	$0.02^{c} \pm 0.00$	$0.19^{a} \pm 0.05$	$0.00^{c} \pm 0.00$	$0.16^{ab} \pm 0.01$	$0.135^{ab} \pm 0.065$	$0.08^{bc} \pm 0.02$
Antral Diameter	$0.02^{e} \pm 0.00$	$0.24^{a} \pm 0.02$	$0.03^{e} \pm 0.00$	$0.11^{cde} \pm 0.00$	$0.03^{e} \pm 0.00$	$0.07^{e} \pm 0.01$
No of cystic follicles	$1.20^{e} \pm 0.20$	$8.50^{a} \pm 0.43$	$2.17^{e} \pm 0.31$	$2.76^{cde} \pm 0.36$	$2.83^{b} \pm 0.47$	$2.18^{ab} \pm 0.37$
No of corpus luteum	5.40 ± 0.51^{cd}	2.33 ± 0.33^{a}	4.9 ± 0.37^{d}	4.14 ± 0.40^{ab}	4.16 ± 0.60^{bc}	4.80 ± 0.37^{bc}
No of healthy follicles	10.40 ± 0.50^{C}	4.17 ± 0.48^{a}	9.50 ± 0.62^{c}	6.29 ± 0.42^{a}	6.33 ± 0.42^{b}	8.20 ± 0.58^{b}

Note: $^{a-e}$ Within the same row, means with different superscripts are significantly different ($p < 0.05$)

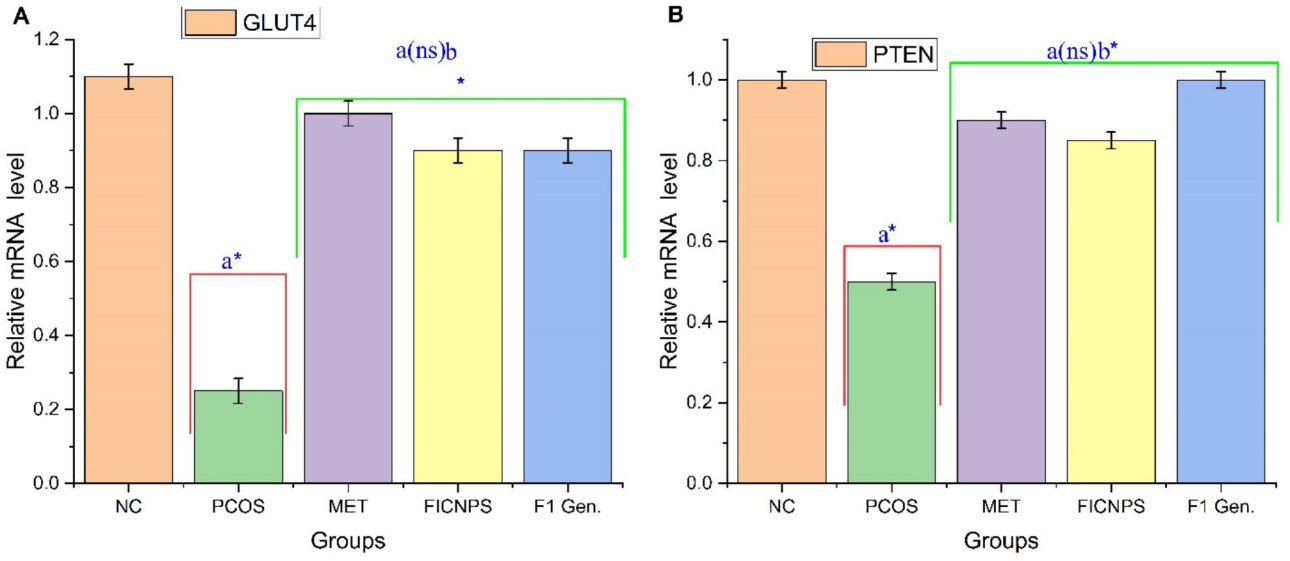

Fig. 9 FICNPs treatment upregulates the expression levels of (**A**) GLUT4 and (**B**) PTEN in the treated group, significantly downregulated in the PCOS rat group. All the experiments were repeated in triplicates. Normal control (NC); a, PCOS group; b, ns; non-significant, asterisk; ($^{*}p < 0.05$)

compared to the control group, whereas groups treated with metformin and FICNPs restored normal mRNA levels (Fig. 9). Additionally, increased expression levels of rno-miR-30c-2-3p, rno-miR-486, and rno-miR-3586-3p were observed in the PCOS environment, whereas a corresponding decrease in rno-miR-146b-5p expression was observed. Notably, intervention with FICNPs or metformin yielded significant outcomes, showing normal miRNA expression patterns in the F1 generation that were alike to those in the control group. These results highlight the possible therapeutic benefits of FICNPs interventions in improving PCOS-associated dysregulation (Fig. 10).

Discussion

PCOS is a predominant condition disturbing woman of reproductive age, with estimates of its global prevalence ranging from 10 to 13%. The load of infertility linked to PCOS has extended significantly over the years, expanding from 6 million prevalent cases in 1990 to 12.13 million in 2019 worldwide. This trend has been observed in most regions and countries [1], emphasizing the need for early and accurate diagnosis of PCOS owing to its strong correlation with infertility and long-term health risks [3, 20]. The presence of oxidative stress can also disrupt normal hormonal signaling and contribute to tissue damage in the ovaries, potentially impacting fertility and overall reproductive health. Hydrogen peroxide (H_2O_2) plays a significant role in oxidative stress within ovarian tissue, particularly affecting granulosa and luteal cells in both rats and human beings [45]. Environmental pollutants like Bisphenol A is also a widely utilized plastic monomer that may disrupt ovarian neuroendocrine, endocrine, and autocrine/paracrine signaling pathways and cases damage to the reproductive system [46].

Although allopathic medicine can manage the symptoms of PCOS, it does not offer a cure, and synthetic drugs often have limited success due to their numerous limitations. The long term usage of these drugs has harmful side effects such as vitamin B12 alterations, hepatotoxicity, acute pancreatitis, and coagulation, inadequate responses, and high costs [47, 48]. Metformin, currently

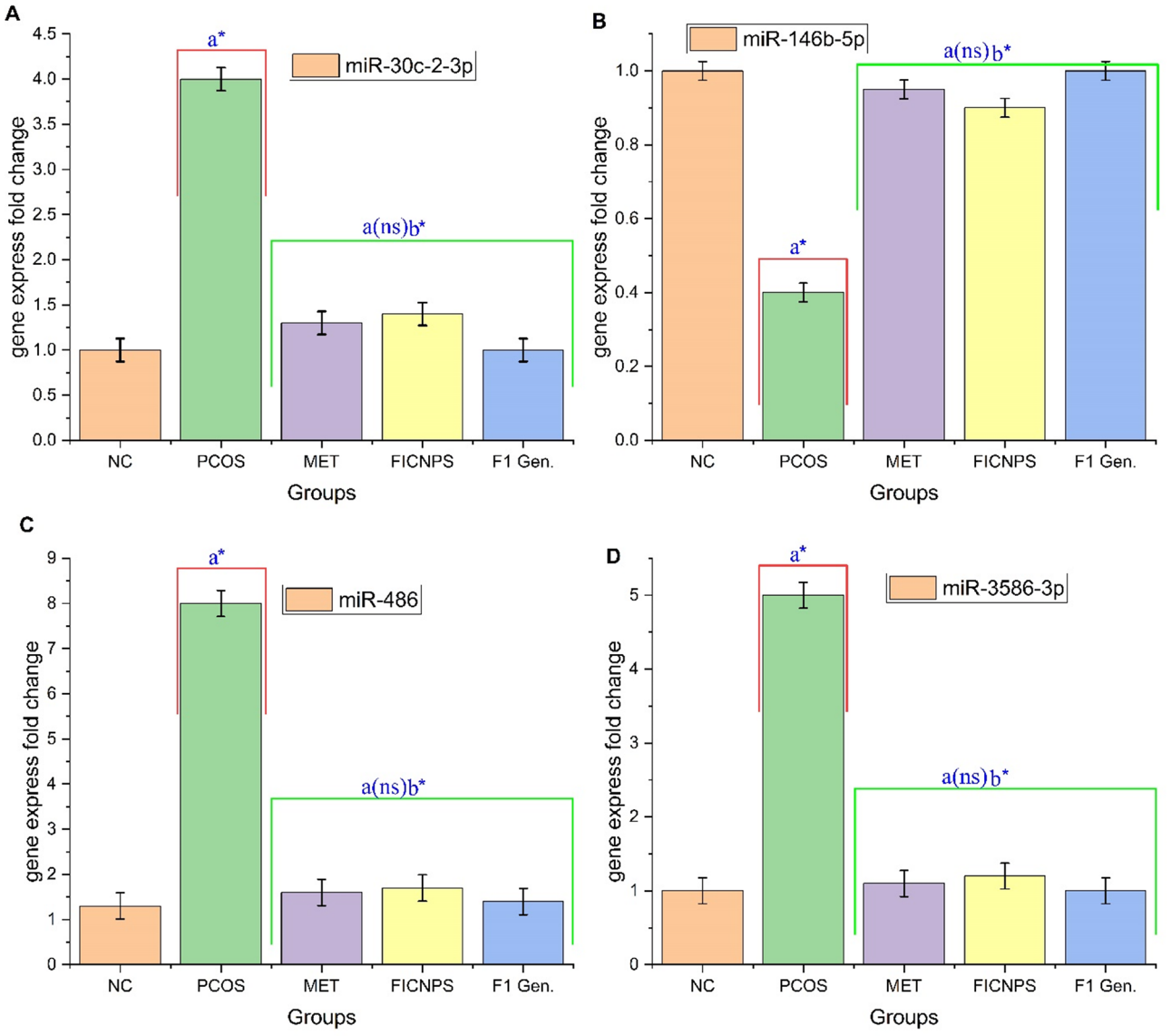

Fig. 10 Differential expression levels of miRNAs participating in PCOS pathogenesis, including, (**A**) miR-30c-2-3p, (**B**) miR-146b-5p, (**C**) miR-486 and (**D**) miR-3586-3p. All the experiments were repeated in triplicates. Normal control (NC); a, PCOS group; b, ns; non-significant, asterisk; ($^{*}p < 0.05$)

the most effective drug for treating PCOS, may also improve oocyte competence [49]. However, metformin does not promote weight loss, despite the possibility that it may be effective in dispersing adipose tissue [50]. The use of metallic nanoparticles (Ag, ZnO, and TiO_2) in disease treatment has significant effects on the female reproductive system, according to Dianova's evaluation of their toxicity on women's reproductive health. Nevertheless, polycystic ovarian syndrome, follicular atresia, inflammation, apoptosis, and necrosis can all be brought on by the buildup of metal nanoparticles in the uterus and ovaries [51].

The development of new natural healing drugs must address the limitations of synthetic therapeutics [49, 50]. Traditional herbal therapies are highly effective due to their gentle impact on body, with fewer or no side effects. Quercetin, a bioactive flavonoid found in plants, influences the hormonal levels of LH and testosterone, which are related to resistance and are essential for steroid synthesis. Recent research has shown that the use of *F. indica* to treat LH has almost returned to normal levels [50, 51]. *F. indica* is known to contain quercetin as one of its primary flavonoid phytoelements. By restoring hormonal equilibrium, lipid profile, and liver function indicators, the plant extract demonstrated beneficial therapeutic effects. *F. indica* treatment eliminated ovarian cysts, decreased body weight, and improved follicular growth. Antioxidant enzyme levels also increased in response to the plant treatments. This study supports that *F. indica* have a beneficial effect on the metabolic and hormonal

abnormalities associated with PCOS [6, 52]. These findings also align with existing research on *Panax ginseng* extract, which has also been shown to improve follicular development due to its pharmacologically active compounds, particularly ginsenosides [42, 53].

Herbal extracts may have a slower efficacy rate and require a longer time to achieve better results for disease treatment. Considering these aspects, in the current study, biomolecules (herbs) combined with chitosan nanoparticles were used for treatment, with no side effects and high efficiency.

Chitosan enhances penetration by releasing the tight bonds between epithelial cells. It facilitates the movement of medications both paracellularly and transcellularly. Chitosan forms a complex through hydrophobic and ionic bonding and interactions with negatively charged mucus [54, 55]. To optimize the outcomes by increasing mucosal absorption, we loaded the plant extract into the TPP-linked Chitosan nanoparticles (CHNPs). Compared to chitosan NPs, FICNPs exhibited improved bio-distribution and reduced toxicity. FICNPs did not trigger any inflammatory response, as indicated by the release of cytokines from squats. Additionally, the bio-distribution of FICNPs was favorable.

After receiving FICNP treatment, the ovarian tissue was reorganized and the healthy follicles were easily seen under a light microscope. There was also clear antrum devoid of cell debris, granulosa cells, and thecal layers in addition to normal follicles. Furthermore, the delivery of FICNPs eliminated polycysts in the ovarian tissues and accelerated the growth of healthy follicles. These findings are reliable with those of a recent study [3], which reported that therapy with "chitosan-propolis nanoparticles (500 mg/kg)" significantly reduced the number of follicular cysts in the ovaries of PCOS rats in comparison to control groups. The results presented in this study are supported by hormonal and histological studies described in the aforementioned research. The findings are consistent with studies demonstrating that coenzyme Q10 administration mitigates cyclophosphamide-induced premature ovarian failure. This treatment avoids premature ovarian failure and promotes folliculogenesis by upregulating the binding of follicle-stimulating hormone (FSH) to its specific receptors (FSHR), which are essential for maintaining ovarian function [56].

The female reproductive system's oocyte maturation and folliculogenesis are two important metabolic and hormonal processes that are regulated by microRNAs (miRNAs) [57, 58]. Changed miRNA levels have been detected in diseases such as oncology, inflammatory conditions, diabetes, and PCOS. Hence, miRNAs are auspicious biomarkers for the timely diagnosis of PCOS. Circulating miRNAs can be obtained from various bodily fluids in women with PCOS, including whole blood, serum, plasma, urine, and follicular fluid [61] Studies have reported significant alterations in miRNA expression in PCOS rat models, particularly in the uterus, which aligns with the broader notion that irregular miRNA expression is associated with a range of diseases [21]. Obesity is associated with elevated miRNA expression in PCOS women, and it has been observed to dramatically decrease the expression of four miRNAs, miR-21, miR-27b, miR-103, and miR-155, in the blood of control women and men [59, 60]. Furthermore, a positive correlation was found between serum testosterone levels and miR-21, miR-27b, and miR-155 after investigating their hormone profiles. Recent analyses have examined the expression levels of four specific microRNAs (miRNAs)," rno-miR-30c-2-3p, rno-miR-146b-5p, rno-miR-486, and rno-miR-3586-3p," in various treated and untreated groups. These findings align with sequencing data and underscore the critical role of miRNAs in the pathophysiology of PCOS. Notably, these miRNAs are regulated by the PI3K/AKT signaling pathway, which is implicated in insulin resistance. Further investigation of the genes GLUT4 and PTEN, both of which are essential for endometrial growth and granulosa cell development, highlights the connection of these insulin-related pathways within the ovarian context [61, 62]. The potential interactions between insulin signaling and FSH and LH pathways suggest that insulin may exert direct modulatory effects on ovarian function. These genes and their associated miRNAs are important for elucidating the mechanisms underlying PCOS pathogenesis [63, 64].

To this point, no comprehensive study has been conducted to assess the impact of *F. indica*-loaded chitosan nanoparticles on the F1 generation in treated groups. In the current study, the treated groups that achieved the most favorable outcomes were analyzed until the next generation using standard male rats. Additionally, hormonal and molecular analyses were performed. The histology of the ovaries in the F1 generation of the FICNPs group was indistinguishable from that of the control group and demonstrated the restoration of ovulation in a rat model of PCOS. The significant reduction in body weight following treatment with extracts loaded with FICNPs was attributed to the efficient absorption of the drug and the elongation of the estrous phase at specific stages.

Conclusion

The current research revealed promising outcomes with the administration of FICNPs, which restored normal estrous cycles, balanced hormone levels, maintained biochemical levels, managed PCOS morphology, and displayed significant anti-infertility effects in PCOS treatment. Quercetin, an active component of *F. indica*, has the potential to alleviate hormonal and metabolic

disturbances associated with PCOS. Our findings suggest that not only do FICNPs protect against PCOS but they also exhibit signs of restoring morphologically damaged ovaries, which regulate the estrous cycle and maintain hormonal equilibrium. This study highlights the potential of biomolecule-loaded chitosan nanoparticles as a side effect-free treatment option for PCOS. Furthermore, this research provides an extensive database of side-effect-free therapies for PCOS related to ovulatory patterns, making it feasible to develop drugs using biomolecule nanotechnology. The models created using rats and mice are more similar to the human PCOS development mechanism, so they are chosen above other rodent/non-rodent models. Given the complexity of PCOS pathophysiology, none of the models studied fully replicates the circumstances associated with PCOS that affect women.

The promising potential of FICNPs as a therapeutic agent for PCOS is proved, further research is needed to enhance their pharmacological properties. Large-scale studies are essential for fully evaluating the efficacy and safety of FICNPs. Once validated, these nanoparticles could offer a novel treatment option for patients with infertility associated with PCOS, minimizing the side effects commonly associated with conventional allopathic medicines.

Acknowledgements
The authors extend their appreciation to the Office of Research and Innovation and Department of Zoology, Government College University, Lahore, Pakistan.

Author contributions
T.Zia and I.Liaqat designed the study. T.Zia, I.Liaqat, S.Alam and A.Saeed completed the experimentation. T.Zia, K. A.Shahzad, D.Fouad and F.S. Ataya analyzed the data. T.Zia and M.H.Lashari prepared the figures and tables. T.Zia wrote the manuscript. I.Liaqat, K.A.Shahzad, M.H.Lashari, D.Fouad, F.S. Ataya proof read the manuscript. All authors approved the manuscript.

Funding
The authors extend their appreciation to Researchers Supporting Project number (RSPD2024R693), King Saud University, Riyadh, Saudi Arabia for funding this work.

Data availability
No datasets were generated or analysed during the current study.

Declarations

Ethical approval
All tests, including those involving animals, were conducted in compliance with international standards and with the consent of the Government College University Lahore Research Ethics Committee, as evidenced by the letter no. GCU/IB/813.

Competing interests
The authors declare no competing interests.

Author details
[1]Physiology and Toxicology Laboratory, Department of Zoology, Government College University Lahore, Lahore, Pakistan
[2]Department of ORL-HNS, Shanghai Fourth People's Hospital, School of Medicine, Tongji University, Shanghai, China
[3]Plasma Medicine and Surgical Implants Center, School of Medicine, Tongji University, Shanghai, China
[4]Department of Zoology, The Islamia University of Bahawalpur, Bahawalpur 63100, Pakistan
[5]Department of Zoology, College of Science, King Saud University, PO Box 22452, Riyadh 11495, Saudi Arabia
[6]Department of Biochemistry, College of Science, King Saud University, PO Box 2455, Riyadh 11451, Saudi Arabia

Received: 11 November 2024 / Accepted: 20 February 2025
Published online: 06 March 2025

References

1. Liu X, Zhang J, Wang S. Global, regional, and National burden of infertility attributable to PCOS, 1990–2019. Hum Reprod. 2024;39(1):108–18.
2. Dapas M, Dunaif A. Deconstructing a syndrome: genomic insights into PCOS causal mechanisms and classification. endocrine reviews. Endocrine Society. 2022; 43, pp 927–65.
3. Hosseini SF, Khodaei F, Hasansagha Z, Khosravizadeh H, Abdollahi M, Azaryan E. Ameliorative Effect of Chitosan-Propolis Nanoparticles on the Estradiol Valerate -Induced PCOS in Rat [Internet]. 2023; Available from: https://www.preprints.org/manuscript/202304.0299/v1
4. Okigbo CC, Gill S, Hall JE. The Hypothalamic-Pituitary Axis in PCOS. In: Polycystic Ovary Syndrome. 2022; pp 73–93.
5. Sirmans SM, Pate KA. Epidemiology, diagnosis, and management of polycystic ovary syndrome. Clin Epidemiol [Internet]. 20131218th ed. 2013; 6:1–13. Available from: https://www.ncbi.nlm.nih.gov/pubmed/24379699
6. Younas A, Hussain L, Shabbir A, Asif M, Hussain M, Manzoor F. Effects of Fagonia indica on Letrozole-Induced Polycystic Ovarian Syndrome (PCOS) in Young Adult Female Rats. Evid Based Complement Alternat Med [Internet]. 20220526th ed. 2022; 2022:1397060. Available from: https://www.ncbi.nlm.nih.gov/pubmed/35664938
7. Fatimah Usman Heriyadi Manan Zulkarnain RA. Effects of Metformin therapy on Anti-Mullerian hormone (AMH) levels in polycystic. Majalah Kedokteran Sriwijaya. 2020; Th. 52,(Nomor 1,).
8. Esan WS, Akintayo CO, Sanya O, Oluwaseun OA, Olubayo G, Adelekan AL. Induction and treatment of polycystic ovary syndrome with plant extract in rats: A systematic review. Eur J Med Plants. 2023;34–48.
9. Liao B, Qiao J, Pang Y. Central Regulation of PCOS: Abnormal Neuronal-Reproductive-Metabolic Circuits in PCOS Pathophysiology. Front Endocrinol (Lausanne) [Internet]. 20210528th ed. 2021; 12:667422. Available from: https://www.ncbi.nlm.nih.gov/pubmed/34122341
10. Matyanga CMJ, Dzingirai B. Clinical Pharmacology of Hormonal Emergency Contraceptive Pills. Int J Reprod Med [Internet]. 20181004th ed. 2018; 2018:2785839. Available from: https://www.ncbi.nlm.nih.gov/pubmed/30402457
11. Reshma BS, Aavula T, Narasimman V, Ramachandran S, Essa MM, Qoronfleh MW. Antioxidant and Antiaging Properties of Agar Obtained from Brown Seaweed Laminaria digitata (Hudson) in D-Galactose-Induced Swiss Albino Mice. Evid Based Complement Alternat Med [Internet]. 20220224th ed. 2022; 2022:7736378. Available from: https://www.ncbi.nlm.nih.gov/pubmed/35251211
12. Khodaeifar F, Fazljou Khaki A, BSM. Investigating the role of hydro-alcoholic extract of Apium graveolens and cinnamon zeylanicum on metabolically change and ovarian oxidative injury in a rat model of polycystic ovary syndrome. Int J Women's Health Reprod Sci. 2019; 7.
13. Dhakad AK, Ikram M, Sharma S, Khan S, Pandey VV, Singh A. Biological, nutritional, and therapeutic significance of Moringa oleifera Lam. Phytother Res [Internet]. 20190827th ed. 2019; 33(11):2870–903. Available from: https://www.ncbi.nlm.nih.gov/pubmed/31453658
14. Soltani M, Moghimian M, Abtahi-Evari SH, Esmaeili SA, Mahdipour R, Shokoohi M. The Effects of Clove Oil on The Biochemical and Histological Parameters, and Autophagy Markers in Polycystic Ovary Syndrome-Model Rats. Int J Fertil Steril [Internet]. 20230401st ed. 2023; 17(3):187–94. Available from: https://www.ncbi.nlm.nih.gov/pubmed/37183845
15. Lakshmi JN, Babu AN, Kiran SSM, Nori LP, Hassan N, Ashames A et al. Herbs as a Source for the Treatment of Polycystic Ovarian Syndrome: A Systematic

Review. BioTech (Basel) [Internet]. 20230103rd ed. 2023;12(1). Available from: https://www.ncbi.nlm.nih.gov/pubmed/36648830
16. Asma Wazir Iqra Kanwal Darakhshan Masroor Mehwish, Khan NF, Tabassum MZ. and A. Phytochemical analysis and fertility enhancement effects of aerial parts of Fagonia Arabica in male and female rats. Pak J Pharm Sci. 2022;35(2).
17. Bonifácio BV, da Silva PB, Aparecido dos Santos Ramos M, Maria Silveira Negri K, Maria Bauab T, Chorilli M. Nanotechnology-based drug delivery systems and herbal medicines: A review. Int J Nanomed. 2013;9:1–15.
18. Bayrami A, Shirdel A, Rahim Pouran S, Mahmoudi F, Habibi-Yangjeh A, Singh R et al. Co-regulative effects of chitosan-fennel seed extract system on the hormonal and biochemical factors involved in the polycystic ovarian syndrome. Mater Sci Eng C Mater Biol Appl [Internet]. 20200811th ed. 2020;117:111351. Available from: https://www.ncbi.nlm.nih.gov/pubmed/32919695
19. Virpal Kaur P. & S. Characterization of bionanoparticles as A medium to prevent Poly- cystic ovary syndrome. Korean J Physiol Pharmacol. 2023; 27(3).
20. Al-Manhel AJ, Al-Hilphy ARS, Niamah AK. Extraction of Chitosan, characterisation and its use for water purification. J Saudi Soc Agricultural Sci. 2018;17(2):186–90.
21. Divya K, Jisha MS. Chitosan nanoparticles Preparation and applications. Environ Chem Lett. 2017;16(1):101–12.
22. Kamada S, Yamamoto Y, Aoki H, Tamura K, Takeda A, Minato S et al. A novel PCOS rat model and an evaluation of its reproductive, metabolic, and behavioral phenotypes. Reprod Med Biol [Internet]. 20211002nd ed. 2022;21(1):e12416. Available from: https://www.ncbi.nlm.nih.gov/pubmed/34934399
23. Anbu AS, Venkatachalam P. Biological macromolecule cross linked TPP–chitosan complex: a novel nanohybrid for improved ovulatory activity against PCOS treatment in female rats. RSC Adv. 2016;6(97):94301–13.
24. Shanker K, Gupta M, Srivastava S, Bawankule D, Pal A, Khanuja S. Determination of bioactive nitrile glycoside(s) in drumstick (Moringa oleifera) by reverse phase HPLC. Food Chem. 2007;105(1):376–82.
25. Kunjachan S, Ehling J, Storm G, Kiessling F, Lammers T. Noninvasive Imaging of Nanomedicines and Nanotheranostics: Principles, Progress, and Prospects. Chem Rev [Internet]. 20150713th ed. 2015;115(19):10907–37. Available from: https://www.ncbi.nlm.nih.gov/pubmed/26166537
26. Zhou M, Wei Z, Qiao H, Zhu L, Yang H, Xia T. Particle size and pore structure characterization of silver nanoparticles prepared by confined Arc plasma. J Nanomater. 2009;2009:1–5.
27. Duraisamy N, Dhayalan S, Shaik MR, Shaik AH, Shaik JP, Shaik B. Green synthesis of Chitosan nanoparticles using of Martynia annua L. Ethanol leaf extract and their antibacterial activity. Cryst (Basel). 2022;12(11).
28. Alwan SH, Al-Saeed MH. Biosynthesized silver nanoparticles (using Cinnamomum zeylanicum bark extract) improve the fertility status of rats with polycystic ovarian syndrome. Biocatal Agric Biotechnol. 2021;38.
29. Sun J, Jin C, Wu H, Zhao J, Cui Y, Liu H et al. Effects of electro-acupuncture on ovarian P450arom, P450c17α and mRNA expression induced by letrozole in PCOS rats. PLoS ONE. 2013;8(11).
30. Pravin PAJ. and TA. Prospective use of Tephrosia Purpurea in remedial treatment of PCOS: study in Wistar rat. J Biol Sci. 2012;3(1).
31. Soumya V, Muzib YI, Venkatesh P. A novel method of extraction of bamboo seed oil (Bambusa bambos Druce) and its promising effect on metabolic symptoms of experimentally induced polycystic ovarian disease. Indian J Pharmacol [Internet]. 2016;48(2):162–7. Available from: https://www.ncbi.nlm.nih.gov/pubmed/27127318
32. Patel R, Shah G. High-fat diet exposure from pre-pubertal age induces polycystic ovary syndrome (PCOS) in rats. Reproduction [Internet]. 20171201st ed. 2018;155(2):141–51. Available from: https://www.ncbi.nlm.nih.gov/pubmed/29196492
33. Haslan MA, Samsulrizal N, Hashim N, Zin N, Shirazi FH, Goh YM, editors. Ficus deltoidea ameliorates biochemical, hormonal, and histomorphometric changes in letrozole-induced polycystic ovarian syndrome rats. BMC Complement Med Ther [Internet]. 20211129th ed. 2021;21(1):291. Available from: https://www.ncbi.nlm.nih.gov/pubmed/34844580
34. Mukilan Ramadoss MV. and AJS. Estradiol valerate dose determination for PCOS induction. Int J Pharm Biol Sci. 2019;9(2).
35. Zhang C, Yu C, Lin Z, Pan H, Li K, Ma H. MiRNAs expression profiling of rat ovaries displaying PCOS with insulin resistance. Arch Gynecol Obstet [Internet]. 20200805th ed. 2020;302(5):1205–13. Available from: https://www.ncbi.nlm.nih.gov/pubmed/32757043
36. Hossain MM, Cao M, Wang Q, Kim JY, Schellander K, Tesfaye D et al. Altered expression of MiRNAs in a dihydrotestosterone-induced rat PCOS model. J Ovarian Res. 2013;6(1).
37. Li C, Chen L, Zhao Y, Chen S, Fu L, Jiang Y, et al. Altered expression of MiRNAs in the uterus from a letrozole-induced rat PCOS model. Gene. 2017;598:20–6.
38. Li Z, Luo Y, Wang C, Han D, Sun W. Circular RNA circblnk promotes osteosarcoma progression and inhibits ferroptosis in osteosarcoma cells by sponging miR-188-3p and regulating GPX4 expression. Oncol Rep. 2023;50(5). https://doi.org/10.3892/or.2023.8629.
39. Abruzzese GA, Ferreira SR, Ferrer MJ, Silva AF, Motta AB. Prenatal Androgen Excess Induces Multigenerational Effects on Female and Male Descendants. Clin Med Insights Endocrinol Diabetes [Internet]. 20230911th ed. 2023;16:11795514231196460. Available from: https://www.ncbi.nlm.nih.gov/pubmed/37705939
40. Farideh Zafari Zangeneh Fatemeh Aminee Mohammad Mahdi Naghizadeh AA. Locus coeruleus lesions and PCOS: role of the central and peripheral sympathetic nervous system in the ovarian function of rat. Iran J Reprod Med. 2012;10(2).
41. Hongsa N, Thinbanmai T, Luesakul U, Sansanaphongpricha K, Muangsin N. A novel modified chitosan/collagen coated-gold nanoparticles for 5-fluorouracil delivery: Synthesis, characterization, in vitro drug release studies, anti-inflammatory activity and in vitro cytotoxicity assay. Carbohydr Polym [Internet]. 20211104th ed. 2022;277:118858. Available from: https://www.ncbi.nlm.nih.gov/pubmed/34893265
42. Honari IRMGH. Antibacterial properties of biologically formed Chitosan nanoparticles using aqueous leaf extract of Ocimum basilicum. Nanomed J. 2016;4(3).
43. Nana Liu Shuyu Wang Xiaowei Zhang Qiufang Zhang Xue, Zhang YM, Qiao LF. and J. Association of the genetic variants of luteinizing hormone, luteinizing hormone receptor and polycystic ovary syndrome. Reproductive Biology Endocrinol. 2012.
44. Fan L, Wang C, Zhan P, Liu Y, editors. miR-141-3p is Poorly Expressed in Polycystic Ovary Syndrome and Correlates with Glucose and Lipid Metabolism. Int J Endocrinol [Internet]. 20211008th ed. 2021;2021:2022938. Available from: https://www.ncbi.nlm.nih.gov/pubmed/34659401
45. Majdi Seghinsara A, Shoorei H, Hassanzadeh Taheri MM, Khaki A, Shokoohi M, Tahmasebi M et al. Panax ginseng Extract Improves Follicular Development after Mouse Preantral Follicle 3D Culture. Cell J [Internet]. 20190220th ed. 2019;21(2):210–9. Available from: https://www.ncbi.nlm.nih.gov/pubmed/30825295
46. Mukhopadhyay R, Prabhu NB, Kabekkodu SP, Rai PS. Review on bisphenol A and the risk of polycystic ovarian syndrome: an insight from endocrine and gene expression. Environmental Science and Pollution Research. Volume 29. Springer Science and Business Media Deutschland GmbH; 2022. pp. 32631–50.
47. Shurrab NT, Arafa ESA, Metformin. A review of its therapeutic efficacy and adverse effects. Volume 17. Obesity Medicine: Elsevier Ltd; 2020.
48. Shantaram Gajanan Khanage TYS and IRB, HERBAL DRUGS FOR THE TREATMENT. OF POLYCYSTIC OVARY SYNDROME (PCOS) AND ITS COMPLICATIONS. Pharm Reson. 2019;2(1).
49. Bailey CJ. Metformin: historical overview. Diabetologia [Internet]. 20170803rd ed. 2017;60(9):1566–76. Available from: https://www.ncbi.nlm.nih.gov/pubmed/28776081
50. Wang R, Mol BW. The Rotterdam criteria for polycystic ovary syndrome: evidence-based criteria? Hum Reprod [Internet]. 20161109th ed. 2017;32(2):261–4. Available from: https://www.ncbi.nlm.nih.gov/pubmed/28119448
51. Shajahan A, Shankar S, Sathiyaseelan A, Narayan KS, Narayanan V, Kaviyarasan V et al. Comparative studies of chitosan and its nanoparticles for the adsorption efficiency of various dyes. Int J Biol Macromol [Internet]. 20170526th ed. 2017;104(Pt B):1449–58. Available from: https://www.ncbi.nlm.nih.gov/pubmed/28554794
52. Dianova L, Tirpak F, Halo M, Slanina T, Massanyi M, Stawarz R et al. Effects of Selected Metal Nanoparticles (Ag, ZnO, TiO(2)) on the Structure and Function of Reproductive Organs. Toxics [Internet]. 20220808th ed. 2022;10(8). Available from: https://www.ncbi.nlm.nih.gov/pubmed/36006138
53. Rahman J, Tareq AM, Hossain MM, Sakib SA, Islam MN, Ali MH et al. Biological Evaluation, DFT Calculations and Molecular Docking Studies on the Antidepressant and Cytotoxicity Activities of Cycas pectinata Buch.-Ham. Compounds. Pharmaceuticals (Basel) [Internet]. 20200903rd ed. 2020;13(9). Available from: https://www.ncbi.nlm.nih.gov/pubmed/32899148
54. Heathcote G, Boothroyd C, Forbes K, Lee A, Gregor M, Luscombe G. Ovulation rate after Metformin and clomiphene vs clomiphene alone in polycystic ovary syndrome (PCOS): A randomized, Double-Blind, Placebo-Controlled trial. Fertility Reprod. 2020;02(01):32–6.

55. Pourteymour Fard Tabrizi F, Hajizadeh-Sharafabad F, Vaezi M, Jafari-Vayghan H, Alizadeh M, Maleki V. Quercetin and polycystic ovary syndrome, current evidence and future directions: a systematic review. J Ovarian Res [Internet]. 20200131st ed. 2020;13(1):11. Available from: https://www.ncbi.nlm.nih.gov/pubmed/32005271
56. Delkhosh A, Delashoub M, Tehrani AA, Bahrami AM, Niazi V, Shoorei H et al. Upregulation of FSHR and PCNA by administration of coenzyme Q10 on cyclophosphamide-induced premature ovarian failure in a mouse model. J Biochem Mol Toxicol [Internet]. 20190926th ed. 2019;33(11):e22398. Available from: https://www.ncbi.nlm.nih.gov/pubmed/31557371
57. Pawar SN, Edgar KJ. Alginate derivatization: a review of chemistry, properties and applications. Biomaterials [Internet]. 20120126th ed. 2012;33(11):3279–305. Available from: https://www.ncbi.nlm.nih.gov/pubmed/22281421
58. Khan I, Saeed K, Khan I, Nanoparticles. Properties, applications and toxicities. Arab J Chem. 2019;12(7):908–31.
59. A glance into the roles. Of MicroRNAs (exosomal and non-exosomal) in polycystic ovary syndrome. Obstetrics and Gynecology Science. Volume 67. Korean Society of Obstetrics and Gynecology; 2024. pp. 30–48.
60. Li Y, Fang Y, Liu Y, Yang X. MicroRNAs in ovarian function and disorders. J Ovarian Res. 2015;8(1).
61. Tamaddon M, Azimzadeh M, Tavangar SM. microRNAs and long non-coding RNAs as biomarkers for polycystic ovary syndrome. J Cell Mol Med [Internet]. 20220106th ed. 2022;26(3):654–70. Available from: https://www.ncbi.nlm.nih.gov/pubmed/34989136
62. Luo Y, Cui C, Han X, Wang Q, Zhang C. The role of miRNAs in polycystic ovary syndrome with insulin resistance. J Assist Reprod Genet [Internet]. 20210106th ed. 2021;38(2):289–304. Available from: https://www.ncbi.nlm.nih.gov/pubmed/33405004
63. Li T, Mo H, Chen W, Li L, Xiao Y, Zhang J et al. Role of the PI3K-Akt Signaling Pathway in the Pathogenesis of Polycystic Ovary Syndrome. Reprod Sci [Internet]. 20160909th ed. 2017;24(5):646–55. Available from: https://www.ncbi.nlm.nih.gov/pubmed/27613818
64. Onal T, Tulay P, Vatansever HS. Does Pten have an impact on oogenesis of PCOS mouse models? Zygote [Internet]. 20221219th ed. 2023;31(1):97–100. Available from: https://www.ncbi.nlm.nih.gov/pubmed/36533329

Publisher's note